

This is the accepted manuscript made available via CHORUS. The article has been published as:

Magnetic properties of two-dimensional hydrocarbon networks of $sp^{\{2\}}$ and $sp^{\{3\}}$ C atoms

Jun-ya Sorimachi and Susumu Okada

Phys. Rev. B **96**, 024103 — Published 13 July 2017

DOI: [10.1103/PhysRevB.96.024103](https://doi.org/10.1103/PhysRevB.96.024103)

Magnetic Properties of 2D Hydrocarbon Networks of sp^2 and sp^3 C Atoms

Jun-ya Sorimachi* and Susumu Okada†

Graduate School of Pure and Applied Sciences, University of Tsukuba,

1-1-1 Tennoudai, Tsukuba, Ibaraki 305-8571, Japan

Abstract

Based on first principles total energy calculations we investigate geometric, electronic, and spin structures in two-dimensional polyacene-based hydrocarbon networks of sp^2 and sp^3 C atoms. Polyacenes connecting adjacent sp^3 atoms form Kagome networks. The networks are stable and retain their covalent topologies up to 2000 K. They possess Kagome flat bands at or near the Fermi level, depending on the size and structure of the polyacene adjoining the sp^3 C atoms. We find that the spin states of the two-dimensional covalent hydrocarbon network are changeable from antiferromagnetic to ferromagnetic by increasing the length of sp^2 C region.

PACS numbers: 73.20.At, 73.22.-f, 73.61.Ph, 75.75.-c

I. INTRODUCTION

Electronic properties of nanomaterials consisting of sp^2 C atoms are sensitive to their network topology, size, dimensionality, and boundary conditions. Thus, the electronic structure of polycyclic hydrocarbon molecules can be classified by size, edge shape, and the number of constituent atoms. Molecules having primarily armchair (cis) edges possess basically symmetric electronic structure with respect to the Fermi level and a moderate energy gap between the highest occupied and the lowest unoccupied states. This gap is inversely proportional to the molecular size¹. However, introducing an imbalance between the numbers of two sublattices in hexagonal networks creates non-bonding states at the Fermi level, leading to the spin polarization. Polymerization of the hydrocarbon molecules causes further variation in the resultant two-dimensional networks²⁻⁴. Their electronic properties depend on the constituent molecule and on the interconnect geometries. For example, graphene nanoribbons exhibit either semiconducting, metallic, or magnetic properties depending on their width and edge shape⁸⁻¹⁴. Besides the hexagonal networks, topological defects such as pentagonal and heptagonal rings make C networks unique in their electronic properties. Fullerenes are the archetypes of nanoscale C network materials containing topological defects. Twelve pentagons embedded in a hollow-cage sp^2 C network render variations in their electronic properties depending on the size and symmetry of their cages⁵⁻⁷.

Hybrid networks of sp^2 and sp^3 C atoms show further variations in their geometric and electronic structures which do not appear in entirely sp^2 C materials. Lacking π electrons, sp^3 C atoms act as spacers for π electron networks while giving structural flexibility, allowing the materials to form three-dimensional structures. Fullerene is constituent unit for constructing such hybrid materials. Polymerized fullerenes can form one-, two-, and three-dimensional covalent networks depending on fullerene cages and the arrangements of the sp^3 C atoms, yielding metallic and semiconducting electronic structures¹⁵⁻¹⁷. Covalent network materials have relatively narrow energy bands around the Fermi level, leading to the peculiar phenomena by injecting electrons or holes into the narrow bands, because sp^3 C atoms decrease the π electron state overlap between adjacent fullerene cages. Propellane and iptycene are representative materials consisting of sp^2 and sp^3 C atoms¹⁸⁻²⁶. In these molecules, three (poly)acenes (sp^2 C units) are adjoined via two sp^3 C atoms situated at their molecular axes. They can form honeycomb networks containing both sp^2 and sp^3 C

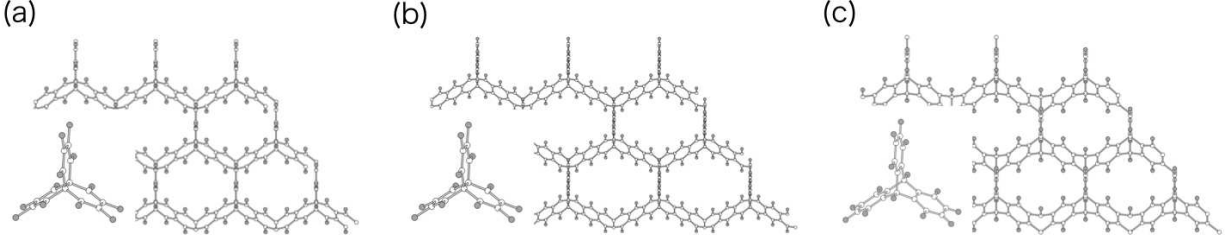


FIG. 1: Optimized structures of propellane networks with (a) C_6 sp^2 and (b) C_{10} sp^2 C atoms, and (c) an iptycene network with C_6 sp^2 C atoms. White and gray balls represent C and H atoms, respectively.

atoms by connecting propellane or iptycene through removal or addition of sp^2 C atoms. In such covalent network materials, π electron transfers within and between the polyacene units may result in electronic structure near the Fermi level which is not seen in entirely sp^2 nanocarbon materials²⁷.

In this paper, we aim to theoretically design two-dimensional covalent hydrocarbon networks consisting of sp^2 and sp^3 C atoms by assembling [4,4,4] propellane and iptycene as constituent molecules. We will investigate their physical properties using density functional theory with the generalized gradient approximation. Our calculations show that the two-dimensional hydrocarbon networks produce a Kagome band at or near the Fermi level, depending on the shape and size of the polyacene inserted between adjacent sp^3 atoms. In a propellane network, because each polyacene has two non-bonding states at the Fermi level, the network exhibits partially filled Kagome flat bands at the Fermi level, leading to spin polarization with various configurations. In an iptycene network, the sp^2 benzene ring results in a semiconductor with Kagome bands just above and below the energy gap. The lowest and second lowest branches of the conduction bands exhibit flat band nature.

II. CALCULATION METHOD

All calculations are based on the density functional theory^{28,29} as implemented in the program package Simulation Tools for Atom TEchnology (STATE)³⁰. We use the generalized gradient approximation with the Perdew-Burke-Ernzerhof functional³¹ to describe the exchange-correlation potential energy among interacting electrons. Ultrasoft pseudopoten-

tials generated by the Vanderbilt scheme are adopted as the interaction between electrons and ions³². Valence wavefunctions and the deficit charge density are expanded in terms of plane wave basis sets with cutoff energies of 25 and 225 Ry, respectively. Integration over the Brillouin zones of the two-dimensional networks were executed by using equidistant $4\times4\times1$ or $2\times2\times1$ \mathbf{k} -meshes, depending on the length of the sp^2 feathers. Lattice parameters and internal atomic structures are fully optimized until the force acting on each atom is less than 1.33×10^{-3} HR/au. The above calculation conditions give sufficient convergence in the geometries and the energetics of the two-dimensional covalent networks of sp^2 and sp^3 C atoms, because the optimized lattice parameters of graphene and diamond are 2.46 and 3.57 Å, respectively, under the condition, which well agree with those of experimental values.

To simulate an isolated two-dimensional hydrocarbon network, we take a large 15.0 Å lattice parameter normal to the network. To investigate thermal stability, a first principles molecular dynamics (MD) simulation was conducted using the velocity scaling method to keep the temperature constant.

III. RESULTS AND DISCUSSION

Figure 1 shows optimized structures of propellane and iptycene hydrocarbon networks. Both molecules have C_3 symmetry with respect to their molecular axis, so that they can form a hexagonal honeycomb covalent network with sp^2 atoms as the interconnect. The honeycomb network is also regarded as a Kagome network of polyacenes which intersect each other at vertexes of sp^3 C atoms. We consider two different propellane networks containing C_6 and C_{10} polyacenes between two sp^3 C atoms. The iptycene network contains a C_6 polyacene between two sp^3 vertexes. The optimized lattice parameters are 8.92 and 13.14 Å for the short (C_6) and elongated (C_{10}) sp^2 C bridges, respectively, for propellane networks. It is 8.98 Å for an iptycene network. In all cases, these networks retain their porous hexagonal covalent structure. Since many porous materials are thermally fragile, the stability of these phases was further investigated using first principles MD simulations. These simulations were conducted under constant temperatures of 1000 and 2000 K for 1 ps simulation times. At all temperatures, all structures retained their covalent network topologies for both sp^2 and sp^3 atoms. Thus, we confirm that the two-dimensional covalent networks proposed here are stable under ambient conditions once they are synthesized using

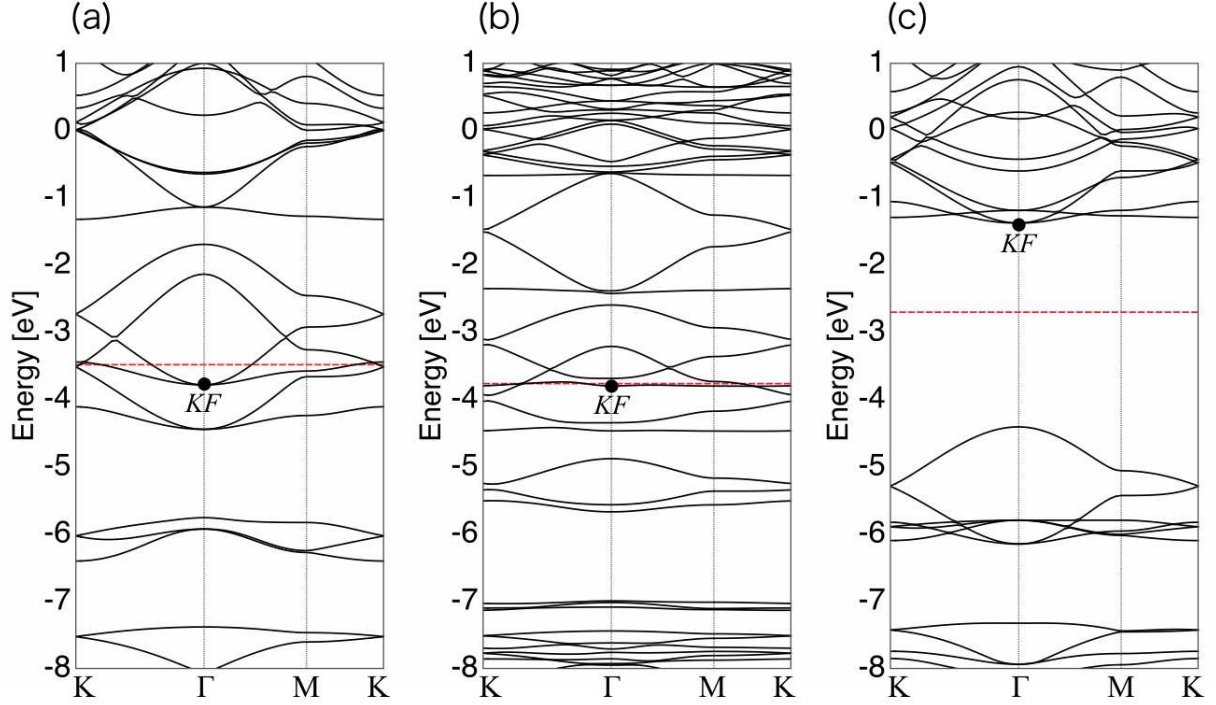


FIG. 2: Electronic structures of the hydrocarbon networks consisting of (a) C_6 propellane vertexes, (b) C_{10} propellane vertexes, and (c) C_6 iptycene vertexes. The red dotted lines indicate Fermi levels. The KF denotes the Kagame flat band state.

the appropriate synthesis procedures.

Figure 2 shows the electronic structures of the hydrocarbon networks of propellane and iptycene vertexes without considering the spin degree of freedom. Characteristics band structures of the Kagome lattice emerges at or near the Fermi level. The propellane networks are metals in which the Fermi level crosses the Kagome flat band, indicating they may exhibit spin polarization owing to the Fermi level instability. In contrast, the iptycene network is a semiconductor with a direct band gap of 3.03 eV at the Γ point. Kagome band character is evident in both the valence band top and the conduction band bottom. The lowest and the second lowest branches of the conduction bands are flat throughout the Brillouin zone.

Flat bands would normally imply the associated wavefunctions are localized at atomic sites. However, these states are not localized but extended throughout the covalent networks. Figure 3 shows the isosurfaces of the wavefucntion of the flat band states at the Γ point labeled KF . Note that the squared wave functions of the KF state in Figs. 3(a) and 3(b) indicate the sum of the squared wave functions of the doubly degenerated states. The

wavefunction distribution corroborates that delicate balance in π electron transfer among the sp^2 C atoms renders the flat band states as the case of usual flat band states in Kagome networks. It is useful to identify which states cause the Kagome band in these covalent hydrocarbon networks. Figure 4 shows energy diagrams of the π electrons bridging sp^3 C atoms. In the propellane network, these are half-filled and doubly degenerate zero energy modes. Furthermore, with increasing the length of polyacene for the case of the C_{10} unit, the sp^2 unit still has doubly degenerated zero energy mode, leading to the metallic nature of the resultant two-dimensional network with propellane vertexes. Thus, two Kagome bands at the Fermi level are ascribed to these zero energy mode of sp^2 networks. In the iptycene network, π electrons form a benzene ring having bonding and antibonding π states just below and above the Fermi level, resulting in the Kagome bands bordering the band gap. The facts indicate that the filling of the Kagome flat band states depend on the atomic structure of the vertex unit of sp^3 C atoms which causes different network topologies of sp^2 C interconnects. Additionally, the width of the Kagome band decreases with increasing sp^2 C length, because of decreasing the electron transfer throughout the network.

It is expected that the Fermi instability will induce spin polarization in the propellane network from the large density of states at the Fermi level. Figure 5 shows the isosurfaces of polarized electron spin in propellane networks containing C_6 and C_{10} sp^2 C atoms. The spin density $\Delta\rho = \rho_\alpha - \rho_\beta$ where ρ_α and ρ_β are the charge densities of α and β spin components, respectively. The propellane network exhibits various metastable spin polarized states. The C_6 network has five metastable spin states summarized in the top row of Table I. Among these five spin states, state (I) is the ground state, wherein the polarized electron spins are antiferromagnetic within each sp^2 unit, and between adjacent sp^2 branches the polarized spins are antiferromagnetically aligned to the extent possible. The frustrated nature of the Kagome lattice causes one of three adjacent pairs exhibits parallel spin coupling. The spin state (II) is the second lowest state. Its spin arrangement between sp^2 units is identical to state (I). However, within the unit, the parallel spin configuration emerges between upper and lower zigzag chains. According to this parallel spin arrangement, the total energy is 3.8 meV above the ground state. In addition to the spin configuration with antiparallel manner, we also find ferromagnetic order throughout the network in the state (III), of which energy is higher by 15.4 meV than that of the ground state. At 21.8 meV above the ground state, the highest energy spin configuration (V) has zero spin density on one of three sp^2 arms.

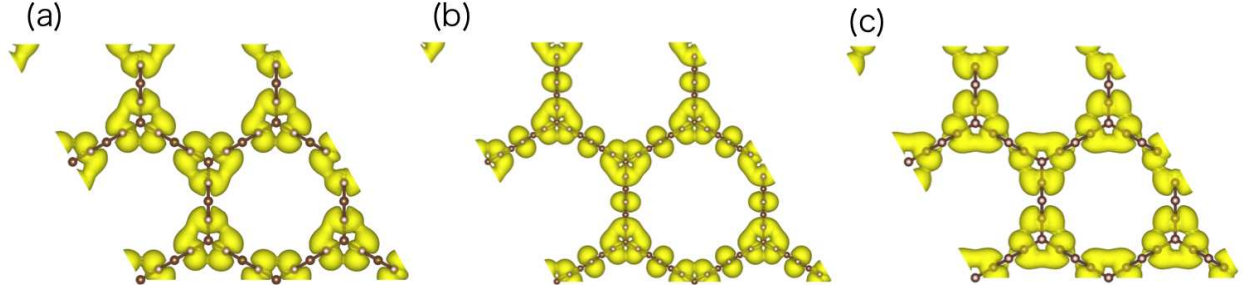


FIG. 3: Isosurfaces of the KF state wavefunction for the (a) C_6 propellane, the (b) C_{10} propellane, and the (c) C_6 ipitycene networks.

TABLE I: Spin densities and relative total energies of the hydrocarbon networks consisting of C_6 and C_{10} with propellane vertexes. Energies are measured from that of the ground state spin configurations.

C_6	I	II	III	IV	V
$\Delta\rho$	0.86	0.88	0.88	0.25	0.25
ΔE [meV]	0	3.8	15.4	17.0	21.8
C_{10}	I	II	III		
$\Delta\rho$	2.00	0.00	0.06		
ΔE [meV]	0	70.4	71.7		

In contrast, in the propellane network containing C_{10} , the ground state is ferromagnetic, with spin ordering within and between the sp^2 C branches. There are two other metastable spin ordered states, both greater than 70 meV above the ground state. In state (II) at 70.4 meV, the spin density on one of three sp^2 arms is absent, giving a set of zigzag chains of alternating ferromagnetic and antiferromagnetic branches. In state (III) at 71.7 meV, the zero spin arms from state (II) are replaced by antiferromagnetic C_{10} sp^2 arms connecting in an overall antiferromagnetic ordering. The substantial differences between C_6 and C_{10} spin orderings means that the length of the sp^2 region can control not only the width of the Kagome band but also the ground state spin configuration across the covalent network.

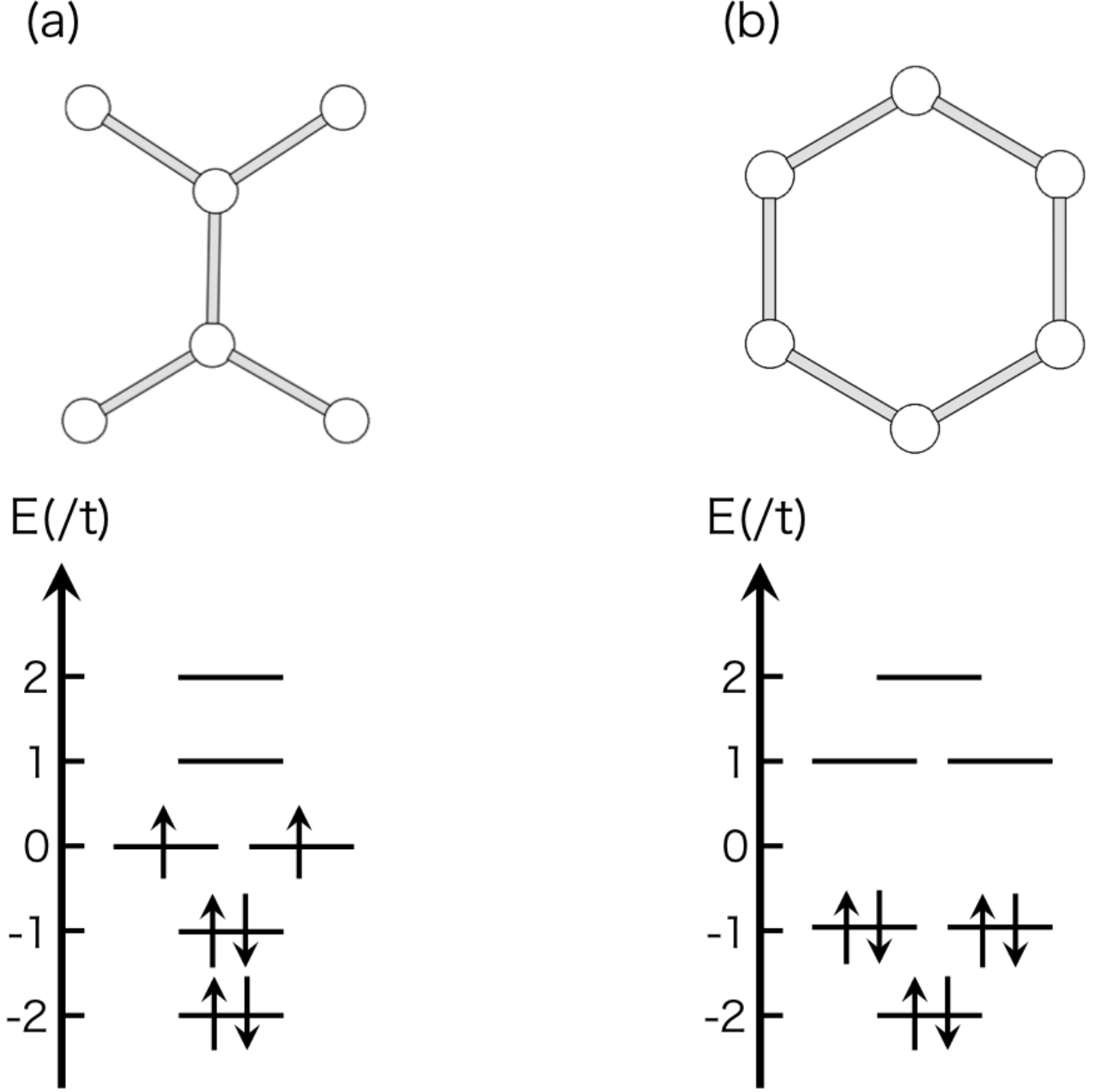


FIG. 4: Energy level diagrams of the sp^2 C unit bridging in (a) propellane and (b) iptycene networks. Energies are scaled by the transfer integral t .

IV. SUMMARY

In this work we investigated the geometric, electronic, and spin structures of two-dimensional hydrocarbon sp^2 and sp^3 C atom networks. Using density functional theory in the generalized gradient approximation, we assembled constituent molecules [4,4,4] propellane and iptycene separately into stable networks. Our calculations find Kagome bands

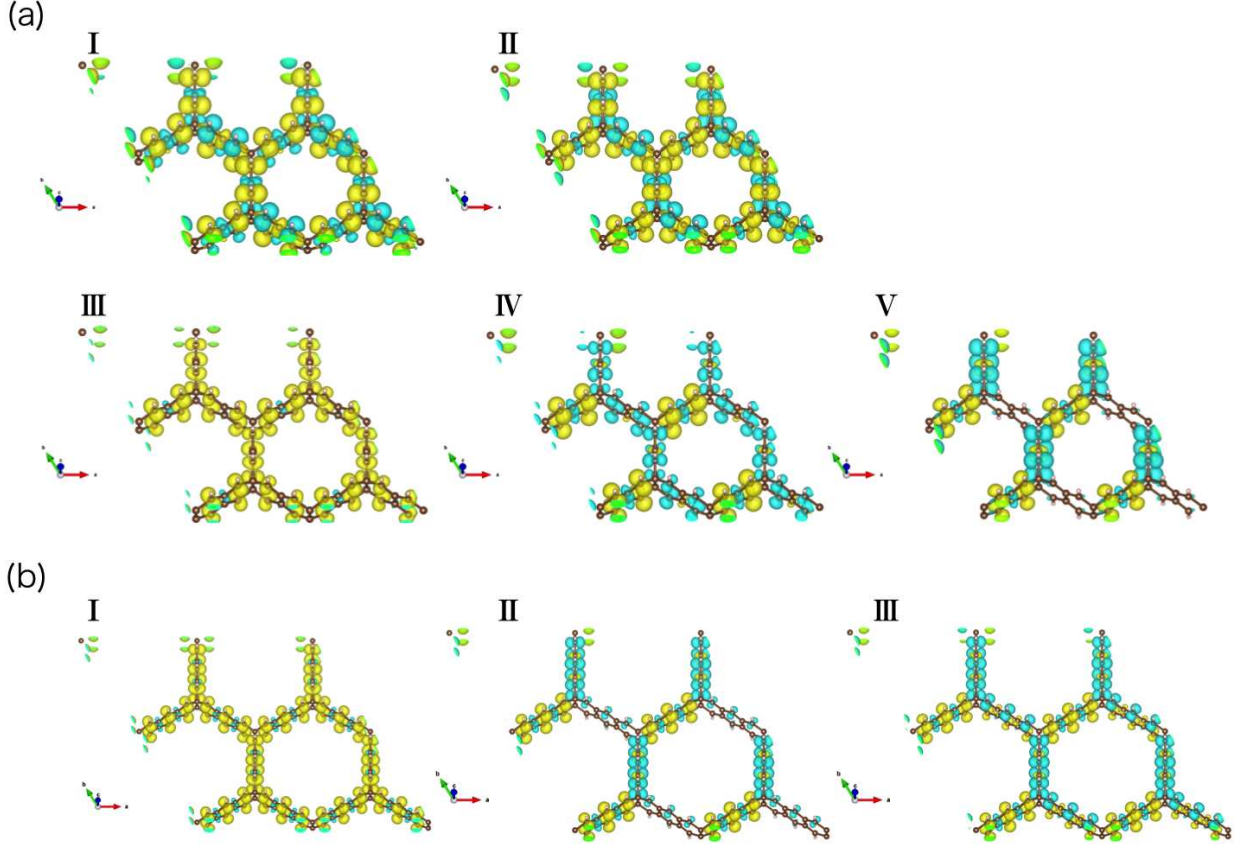


FIG. 5: Polarized spin states of the propellane networks with (a) C_6 sp^2 and (b) C_{10} sp^2 atoms. Yellow and blue isosurfaces indicate α and β spin densities, respectively.

at or near the Fermi level depending on the polyacene branches. In propellane networks, since each sp^2 C moiety possesses two non-bonding states at the Fermi level, the electronic structure of the network has partially filled Kagome flat bands at the Fermi level leading to spin polarization. Electron spins prefer antiferromagnetic coupling between and within the sp^2 moieties, leading to various spin configurations because of the frustrated nature of Kagome lattices for the antiferromagnetic spin interaction. By increasing the length of the polyacene structure, the Kagome band decreases its width and leads to ferromagnetic order throughout the network as a ground state. In iptycene networks, the benzene ring produces a semiconducting electronic structure with a direct band gap at the Γ point. Kagome bands occur just above and below the band gap, and both the lowest and the second lowest branches of the conduction bands are flat. Because of the 120-degree corner at propellane and iptycene vertexes, π states substantially overlap between adjacent sp^2 moieties, leading to their extended character throughout the network. Recent experiments reported the polymerized

and oligomerized networks of iptycene as the networks consisting of sp^2 and sp^3 C atoms^{33,34}. Furthermore, a honeycomb architecture composed of triptycene connected via NH-bridges³⁵ has been synthesized. Based on our theoretical prediction and the experimental synthesis of precursors, the hydrocarbon network of sp^2 and sp^3 atoms are the promising examples of the Kagome network in which the filling of the flat band states and band width are tunable by controlling the atomic arrangements of sp^2 and sp^3 C atoms. **Structural identifications of the hybrid networks of sp^2 and sp^3 C atoms may be confirmed using the ^{13}C -NMR experiment for determining the ratio of sp^2 and sp^3 C and using the photo-absorption experiment for observing the substantial peaks associated with the Kagome flat band states.**

Acknowledgments

This work was supported by CREST from the Japan Science and Technology Agency, by JSPS KAKENHI Grant Numbers JP17H01069, JP16H00898, and JP16H06331 from Japan Society For the Promotion of Science, and by the Joint Research Program on Zero-Emission Energy Research, Institute of Advanced Energy, Kyoto University. Portions of the calculations were performed on an NEC SX-Ace at the Cybermedia Center at Osaka University and on an SGI ICE XA/UV at the Institute of Solid State Physics, The University of Tokyo.

* Electronic address: `jsorimachi@comas.frsc.tsukuba.ac.jp`

† Electronic address: `sokada@comas.frsc.tsukuba.ac.jp`

¹ E. Clar, *The Aromatic Sextet* (John Wiley and Sons, London, U.K. 1972).

² N. Shima and H. Aoki, Phys. Rev. Lett. **71**, 4389 (1993).

³ M. Maruyama, N. T. Cuong, and S. Okada, Carbon **109**, 755 (2016).

⁴ M. Maruyama and S. Okada, Appl. Phys. Express **6**, 095101 (2013)

⁵ B. L. Zhang, C. Z. Wang, and K. M. Ho, Chem. Phys. Lett. **193**, 225 (1992).

⁶ B. L. Zhang, C. Z. Wang, K. M. Ho, C. H. Xu, and C. T. Chan, J. Chem. Phys. **98**, 3095 (1993).

⁷ S. Saito, S. Okada, S.I. Sawada, and N. Hamada, Phys. Rev. Lett. **75**, 685 (1995).

- ⁸ M. Fujita, K. Wakabayashi, K. Nakada, and K. Kusakabe, J. Phys. Soc. Jpn. **65**, 1920 (1996).
- ⁹ K. Nakada, M. Fujita, G. Dresselhaus, and M.S. Dresselhaus, Phys. Rev. B **54**, 17954 (1996).
- ¹⁰ Y.-W. Son, M.L. Cohen, and S.G. Louie, Phys. Rev. Lett. **97**, 216803 (2006).
- ¹¹ Y. Miyamoto, K. Nakada, and M. Fujita, Phys. Rev. B **59**, 9858 (1999).
- ¹² Y. Kobayashi, K.I. Fukui, T. Enoki, and K. Kusakabe, Phys. Rev. B **73**, 125415 (2006).
- ¹³ S. Okada and A. Oshiyama, Phys. Rev. Lett. **87**, 146803 (2001).
- ¹⁴ A. Yamanaka and S. Okada, Carbon **96**, 351 (2016).
- ¹⁵ S. Okada and S. Saito, Phys. Rev. B **55**, 4039 (1997).
- ¹⁶ S. Okada and S. Saito, Phys. Rev. B **59**, 1930 (1999).
- ¹⁷ S. Okada, S. Saito, and A. Oshiyama, Phys. Rev. Lett. **83**, 1986 (1999).
- ¹⁸ O. Ermer, R. Gerdil, and J. D. Dunitz, Helv. Chim. Acta. **54**, 2476 (1971).
- ¹⁹ J. Altman, D. Becker, D. Ginsburg, and H. J. E. Leewenthal, Tetrahedron Lett. **8**, 757 (1967).
- ²⁰ R. G. D. Taylor, C. G. Bezzu, M. Carta, K. J. Msayib, J. Walker, R. Short, B. M. Kariuki, and N. B. McKeown, Chem. Euro. J. **22**, 2466 (2016).
- ²¹ N. V. Krainyukova and E. N. Zubarev, Phys. Rev. Lett. **116**, 055501 (2016).
- ²² H. Hart, S. Shamouilian, and Y. Takehira, J. Org. Chem. **46**, 4427 (1981).
- ²³ C.-F. Chen, Chem. Commun. **47**, 1674 (2011).
- ²⁴ T. M. Swager, Acc. Chem. Res. **41**, 1181 (2008).
- ²⁵ M. Mastalerz and I. M. Oppel, Angew. Chem. Int. Ed. **51**, 5252 (2012).
- ²⁶ P. Kissel, D. J. Murray, W. J. Wulftange, V. J. Catalano, and B. T. King, Nat. Chem. **6**, 774 (2014).
- ²⁷ T. Kawai, S. Okada, Y. Miyamoto, and A. Oshiyama, Phys. Rev. B **72**, 035428 (2005).
- ²⁸ P. Hohenberg and W. Kohn, Phys. Rev. **136**, B864 (1964).
- ²⁹ W. Kohn and L. J. Sham, Phys. Rev. **140**, A1133 (1965).
- ³⁰ Y. Morikawa, K. Iwata, and K. Terakura, Appl. Surf. Sci. **169-170**, 11 (2001).
- ³¹ J. P. Perdew, K. Burke, and M. Ernzerhof, Phys. Rev. Lett. **77**, 3865 (1996).
- ³² D. Vanderbilt, Phys. Rev. B **41**, 7892 (1990).
- ³³ D. F. Perepichka, M. Bendikov, H. Meng, and F. Wudl, J. Am. Chem. Soc. **125**, 10190 (2003).
- ³⁴ J.-S. Yang, J.-L. Yan, C.-Y. Hwang, S.-Y. Chiou, K.-L. Liao, H.-H. G. Tsai, G.-H. Lee, and S.-M. Peng, J. Am. Chem. Soc. **128**, 14109 (2006).
- ³⁵ M. Xue and C.-F. Chen, Chem. Commun. **47**, 2318 (2011).